International Journal of Engineering Science 90 (2015) 76–85

Contents lists available at ScienceDirect

International Journal of Engineering Science

journal homepage: www.elsevier.com/locate/ijengsci

Computational evaluation of effective stress relaxation behavior of polymer composites

Tian Tang *, Sergio D. Felicelli

Department of Mechanical Engineering, The University of Akron, Akron, OH 44325, United States

ARTICLE INFO

Article history:
Received 7 December 2014
Received in revised form 3 February 2015
Accepted 14 February 2015
Available online 9 March 2015

Keywords:
Viscoelastic behavior
Polymer composite
Micromechanics
VAMUCH
Effective stress relaxation stiffness

ABSTRACT

This paper presents a micromechanics model to characterize the effective stress relaxation stiffness of polymer composites. The linear viscoelastic behavior of polymer material was modeled by hereditary integral. The proposed model was established based on the variational asymptotic method for unit cell homogenization (VAMUCH). All computations with this model were accomplished in the time domain, hence the Laplace transform and inversion commonly used for linear viscoelastic composites are not needed in this theory. The accuracy and efficiency of the proposed model were verified by comparing with the results and utilization of finite element models developed using ABAQUS.

1. Introduction

Polymer matrix composites, which are composed of a variety of short or long fibers bound together by organic polymer matrix, have been widely utilized in many engineering areas. Due to the viscoelastic behavior of the polymer matrix, polymer matrix composites exhibit evidently viscoelastic behavior, in which the magnitude of stress and strain are time and temperature dependent. The viscoelasticity phenomenon of polymer composites results from the long molecular chains of the polymer matrix. The creep and stress relaxation responses of polymer composites seriously restrict the advanced composites structures expected to operate for long period of time on many applications (Barbero, 1994).

Micromechanics models are the major tools to characterize the viscoelastic behavior of polymer composites (Aboudi, 2000; Hashin, 1983; Nemat-Nasser & Hori, 1993). Hashin (1965, 1970, 1970) was the first one developing the correspondence principle, which showed that the effective relaxation and creep functions of viscoelastic heterogeneous media are related to the effective elastic moduli of elastic heterogeneous media by the correspondence principle of the theory of linear viscoelasticity. Park and Schapery (1999) developed an efficient and accurate numerical method of interconversion between linear viscoelastic material functions based on a Prony series representation. Their method is straightforward and applicable to interconversion between modulus and compliance functions in time, frequency, and Laplace transform domains. The most common methodology for characterizing the viscoelastic behavior of polymer composites is to apply the Laplace transform and Laplace inversion, where the correspondence principle was applied (Barbero & Luciano, 1995; Christensen, 1979; Haasemann & Ulbricht, 2009; Megnis, Varna, Allen, & Holmberg, 2001; Li, Gao, & Roy, 2006; Schapery, 1967; Li et al., 2006; Wang & Weng, 1992; Yancey & Pindera, 1990). Brinson and Lin (2003) and Fisher and Brinson (2003) employed the finite element method to analyze the two-phase and three-phase viscoelastic composites in the Laplace transformed

* Corresponding author. Tel.: +1 330 972 7672.
E-mail address: tiantang1991@gmail.com (T. Tang).

http://dx.doi.org/10.1016/j.ijengsci.2015.02.003
0020-7225/

domain, respectively, and verified the results with the Mori–Tanaka model (Benveniste, 1987; Mori & Tanaka, 1973). Levin and Sevostianov (2005) proposed an analytical approach for micromechanics modeling of the effective viscoelastic behavior of composites in which the fraction-exponential operator was used to describe the viscoelastic properties of the constituents. Recently, commercial finite element software ABAQUS was applied to predict the stress relaxation response (Abadi, 2009) and creep response (Naik, Abolfathi, Karami, & Ziejewski, 2008) of fiber reinforced polymer matrix composites considering a unit cell subjected to periodic boundary conditions.

The objective of this paper is to develop a micromechanics model to characterize the effective stress relaxation stiffness of viscoelastic polymer composites. The proposed model is an extension of VAMUCH (variational asymptotic method for unit cell homogenization) for effective elastic properties (Yu & Tang, 2007). The effective viscoelastic responses of polymer composites were calculated in time domain. Hence the commonly used Laplace transform and inversion are not required in this theory. Furthermore, the proposed model calculates simultaneously the complete set of effective stress relaxation stiffness so that it is far more convenient than conventional finite element approaches with which multiple running are required on multiple loading and boundary conditions. The accuracy and efficiency of the present modeling technique were validated through the comparison with the results and utilization of finite element models developed based on ABAQUS.

2. Theoretical equations of stress relaxation stiffness of linear viscoelastic materials

Based on the Boltzmann superposition principle, the constitutive equations for the linear viscoelastic material can be expressed in the time domain in the following way,

$$\sigma_{ij}(t) = \int_{-\infty}^{t} C_{ijkl}(t-\tau)\dot{\varepsilon}_{kl}(\tau)d\tau \tag{1}$$

where $C_{ijkl}(t)$ is the stress relaxation stiffness; $\dot{\varepsilon}_{kl}(\tau)$ is the strain rate; $\sigma_{ij}(t)$ is the stress tensor.

The stress relaxation tests are performed at constant strains, which means

$$\varepsilon_{kl}(t) = \begin{cases} 0 & t < 0 \\ \varepsilon_{kl}^{\mathrm{cst}} & t \geqslant 0 \end{cases} \tag{2}$$

where "cst" means constant values that do not vary with time but may change with position.

Eq. (2) implies: $\lim_{t\to-\infty}\varepsilon_{kl}(t) = 0$.

Then applying the integral by parts to Eq. (1), we can obtain

$$\sigma_{ij}(t) = \left(C_{ijkl}(0) + \int_0^t \frac{\partial C_{ijkl}(t-\tau)}{\partial(t-\tau)}\mathrm{d}\tau\right)\varepsilon_{kl}^{\mathrm{cst}} = C_{ijkl}(t)\varepsilon_{kl}^{\mathrm{cst}} \tag{3}$$

Eq. (3) implies that the instantaneous stress values are dependent on the instantaneous values of stress relaxation coefficients instead of history effects when the linear viscoelastic materials are subjected to constant strain loading.

3. Micromechanics formulations for effective stress relaxation stiffness

Consider a multiphase viscoelastic composite that is an assembly of many periodic unit cells (UCs). The microstructure of the multiphase composite is illustrated in Fig. 1. Two coordinate systems including $\boldsymbol{x} = (x_1, x_2, x_3)$ and $\boldsymbol{y} = (y_1, y_2, y_3)$ are employed to facilitate the micromechanics formulations. We use x_i as the global coordinates to describe the macroscopic structure and y_i parallel to x_i as the local coordinates to describe the UC (Here and throughout the paper, Latin indices assume 1–3 and repeated indices are summed over their range except where explicitly indicated). We choose the origin of the local coordinate system y_i to be the geometric center of UC.

3.1. Effective stress relaxation stiffness of linear viscoelastic composites

The Eq. (3) may be derived from the following transient potential energy density functional,

$$U(t) = \frac{1}{2}C_{ijkl}(t)\varepsilon_{ij}^{\mathrm{cst}}\varepsilon_{kl}^{\mathrm{cst}} \tag{4}$$

such that

$$\sigma_{ij}(t) = \frac{\partial U(t)}{\partial \varepsilon_{ij}^{\mathrm{cst}}} \tag{5}$$

The effective stress relaxation stiffness of the linear viscoelastic composites can be defined in the following ways,

$$\bar{\sigma}_{ij}(t) = C_{ijkl}^{*}(t)\bar{\varepsilon}_{kl}^{\mathrm{cst}} \tag{6}$$

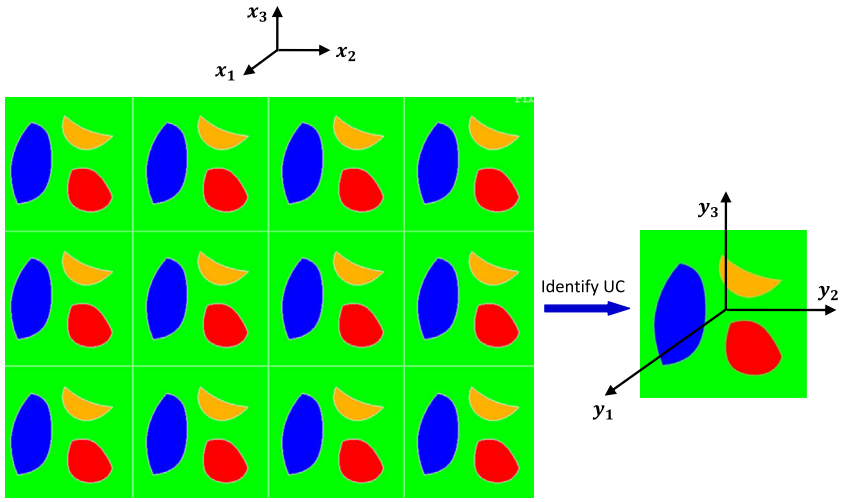

Fig. 1. A sketch of periodic heterogeneous materials (only two-dimensional (2D) unit cell (UC) is drawn for clarity).

$$\frac{1}{\Omega}\int_{\Omega}\frac{1}{2}C_{ijkl}(t)\varepsilon_{ij}(t)\varepsilon_{kl}(t)d\Omega=\frac{1}{2}C^{*}_{ijkl}(t)\bar{\varepsilon}^{\mathrm{cst}}_{ij}\bar{\varepsilon}^{\mathrm{cst}}_{kl} \tag{7}$$

where "over-bar" indicates variables which are used in the macroscopic analysis of homogenized materials and Ω is the volume of unit cell, such that

$$\bar{\varepsilon}^{\mathrm{cst}}_{ij}=\frac{1}{\Omega}\int_{\Omega}\varepsilon_{ij}(t)\mathrm{d}\Omega \tag{8}$$

$$\bar{\sigma}_{ij}(t)=\frac{1}{\Omega}\int_{\Omega}\sigma_{ij}(t)\mathrm{d}\Omega \tag{9}$$

Although the externally applied mechanical strain to the viscoelastic composites are kept constant as $\bar{\varepsilon}^{\mathrm{cst}}_{ij}$, the local strain $\varepsilon_{ij}(t)$ and local stress $\sigma_{ij}(t)$ within unit cell vary with time due to the stress relaxation of linear viscoelastic polymer. Superscripts "*" in Eqs. (6), (7) denote the effective properties whose calculations are determined by the micromechanics model one employs.

3.2. VAMUCH model

The proposed model for effective stress relaxation stiffness of linear viscoelastic composites is an extension of the variational asymptotic method for unit cell homogenization (VAMUCH) for elastic composites (Yu & Tang, 2007). Following a similar derivation procedure as in Yu and Tang (2007), we can obtain a variational statement which govern the micromechanics model. The final theory of VAMUCH for homogenizing linear viscoelastic heterogeneous materials subjected to constant strains can be obtained by minimizing

$$\Pi_{\Omega}=\frac{1}{2\Omega}\int_{\Omega}C_{ijkl}(t)\left[\bar{\varepsilon}^{cst}_{ij}+\chi_{(i|j)}\right]\left[\bar{\varepsilon}^{cst}_{kl}+\chi_{(k|l)}\right]d\Omega \tag{10}$$

subjected to periodic constraints $\chi_i^{+j}=\chi_i^{-j}$ for $i,\ j=1,2,3$ with $\chi_i^{+j}=\chi_i|_{y_j=d_j/2}$ and $\chi_i^{-j}=\chi_i|_{y_j=-d_j/2}$. Here, χ_i is the commonly called fluctuating function and d_j is the size of the unit cell, $\bar{\varepsilon}^{cst}_{ij}$ is the global constant strains.

We introduced the following matrix notations:

$$\bar{\epsilon}=\lfloor\bar{\varepsilon}^{cst}_{11}\quad 2\bar{\varepsilon}^{cst}_{12}\quad \bar{\varepsilon}^{cst}_{22}\quad 2\bar{\varepsilon}^{cst}_{13}\quad 2\bar{\varepsilon}^{cst}_{23}\quad \bar{\varepsilon}^{cst}_{33}\rfloor^{T} \tag{11a}$$

$$\epsilon_1=\lfloor\hat{\varepsilon}_{11}(t)\quad 2\hat{\varepsilon}_{12}(t)\quad \hat{\varepsilon}_{22}(t)\quad 2\hat{\varepsilon}_{13}(t)\quad 2\hat{\varepsilon}_{23}(t)\quad \hat{\varepsilon}_{33}(t)\rfloor^{T} \tag{11b}$$

where

$$\bar{\varepsilon}^{cst}_{ij}=\frac{1}{2}\left[\frac{\partial v_i(\boldsymbol{x})}{\partial x_j}+\frac{\partial v_j(\boldsymbol{x})}{\partial x_i}\right] \tag{12a}$$

$$\hat{\varepsilon}_{ij}(t) = \chi_{(i|j)} = \frac{1}{2}\left[\frac{\partial \chi_i(t;\boldsymbol{x};\boldsymbol{y})}{\partial y_j} + \frac{\partial \chi_j(t;\boldsymbol{x};\boldsymbol{y})}{\partial y_i}\right] \tag{12b}$$

where $v_i(\boldsymbol{x}) = \frac{1}{\Omega}\int_\Omega [u_i(t;\boldsymbol{x};\boldsymbol{y})]d\Omega$ with $u_i(t;\boldsymbol{x};\boldsymbol{y})$ being the local displacement vectors that is expressed as: $u_i(t;\boldsymbol{x};\boldsymbol{y}) = v_i(\boldsymbol{x}) + y_j\frac{\partial v_i}{\partial x_j} + \chi_i(t;\boldsymbol{x};\boldsymbol{y})$.

Then the matrix ϵ_1 in Eq. (11b) can also be written as

$$\epsilon_1 = \begin{bmatrix} \frac{\partial}{\partial y_1} & 0 & 0 \\ \frac{\partial}{\partial y_2} & \frac{\partial}{\partial y_1} & 0 \\ 0 & \frac{\partial}{\partial y_2} & 0 \\ \frac{\partial}{\partial y_3} & 0 & \frac{\partial}{\partial y_1} \\ 0 & \frac{\partial}{\partial y_2} & \frac{\partial}{\partial y_3} \\ 0 & 0 & \frac{\partial}{\partial y_3} \end{bmatrix} \begin{Bmatrix} \chi_1 \\ \chi_2 \\ \chi_3 \end{Bmatrix} \equiv \Gamma_h \chi \tag{13}$$

where Γ_h is an operator matrix and χ is a column matrix containing the three components of the fluctuation functions. If we discretize χ using finite elements as

$$\chi(x_i;y_i) = S(y_i)\boldsymbol{\chi}(x_i) \tag{14}$$

where S representing the shape functions (in assemble sense excluding the constrained node and slave nodes) and $\boldsymbol{\chi}$ column matrix of the nodal value of the fluctuation functions for all active nodes. Substituting Eqs. (11)–(14) into Eq. (10), we obtain a discretized version of the functional as

$$\Pi_\Omega = \frac{1}{2\Omega}\left(\boldsymbol{\chi}^T E\boldsymbol{\chi} + 2\boldsymbol{\chi}^T D_{h\varepsilon}\bar{\epsilon} + \bar{\epsilon}^T D_{\varepsilon\varepsilon}\bar{\epsilon}\right) \tag{15}$$

where

$$E = \int_\Omega (\Gamma_h S)^T D(\Gamma_h S)d\Omega \quad D_{h\varepsilon} = \int_\Omega (\Gamma_h S)^T D d\Omega \quad D_{\varepsilon\varepsilon} = \int_\Omega D d\Omega \tag{16}$$

with D as the 6×6 material matrix condensed from the fourth-order stress relaxation stiffness tensor $C_{ijkl}(t)$. Note that the stress relaxation stiffness tensor of linear elastic materials is equal to the elastic stiffness tensor C^e_{ijkl}, which is time-independent. Minimizing Π_Ω in Eq. (15), we obtain the following linear system:

$$E\boldsymbol{\chi} = -D_{h\varepsilon}\bar{\epsilon} \tag{17}$$

The fluctuation function $\boldsymbol{\chi}$ is linearly proportional to $\bar{\varepsilon}$, which means the solution can be written as

$$\boldsymbol{\chi} = \boldsymbol{\chi}_0\bar{\epsilon} \tag{18}$$

Substituting Eq. (18) into Eq. (15), we can calculate the free energy density of the UC as

$$\Pi_\Omega = \frac{1}{2\Omega}\bar{\epsilon}^T\left(\boldsymbol{\chi}_0^T D_{h\varepsilon} + D_{\varepsilon\varepsilon}\right)\bar{\epsilon} = \frac{1}{2}\bar{\epsilon}^T D^*\bar{\epsilon} \tag{19}$$

Clearly D^* is a 6×6 effective material matrix containing the effective stress relaxation stiffness coefficients.

4. Model verifications

In this section, the VAMUCH model was used to predict the effective stress relaxation stiffness $C^*_{ijkl}(t)$ of glass fiber reinforced polymer matrix composites. The glass fibers are of circular shape and in square array. In order to verify the accuracy and efficiency of the VAMUCH model, the finite element unit cell models for effective stress relaxation stiffness were also developed based on ABAQUS.

4.1. Material properties of constituents

Glass fiber The glass fibers are isotropic and linear elastic materials. The material properties of the glass fiber are shown in Table 1.

Polymer The elastic relaxation modulus of the isotropic and linear viscoelastic polymer materials can be expressed using Prony series as

$$E(t) = E_0\left(1 - \sum_{k=1}^{n} g_k\left(1 - e^{-t/\tau_k}\right)\right) \tag{20}$$

Table 1
Elastic properties of glass fibers (Megnis et al., 2001).

	Young's modulus E (MPa)	Poisson's ratio v
Glass fiber	80,000	0.3

where E_0 is the instantaneous Young's modulus; g_k is dimensionless modulus and τ_k is the time relaxation material parameter. For simplicity, we considered a special case, namely, $n = 1,\ g_1 = 0.5$, and $\tau_1 = 30$, such that Eq. (20) is reduced to

$$E(t) = 0.5E_0\left(1 + e^{-t/\tau_1}\right) \tag{21}$$

where $E_0 = 8000$ MPa. The Poisson's ratio of the polymer is assumed to be constant $v = 0.4$.

4.2. ABAQUS finite element unit cell models

The effective properties of fiber reinforced composites with the fibers being in square array possess square symmetry. Their effective stress relaxation stiffness matrix can be expressed as

$$\begin{Bmatrix} \bar{\sigma}_{11}(t) \\ \bar{\sigma}_{22}(t) \\ \bar{\sigma}_{33}(t) \\ \bar{\sigma}_{23}(t) \\ \bar{\sigma}_{12}(t) \\ \sigma_{13}(t) \end{Bmatrix} = \begin{bmatrix} C^*_{11}(t) & C^*_{12}(t) & C^*_{12}(t) & 0 & 0 & 0 \\ C^*_{12}(t) & C^*_{22}(t) & C^*_{23} & 0 & 0 & 0 \\ C^*_{12}(t) & C^*_{23}(t) & C^*_{22} & 0 & 0 & 0 \\ 0 & 0 & 0 & C^*_{44}(t) & 0 & 0 \\ 0 & 0 & 0 & 0 & C^*_{55}(t) & 0 \\ 0 & 0 & 0 & 0 & 0 & C^*_{55}(t) \end{bmatrix} \begin{Bmatrix} \bar{\varepsilon}^{cst}_{11} \\ \bar{\varepsilon}^{cst}_{22} \\ \bar{\varepsilon}^{cst}_{33} \\ \bar{\gamma}^{cst}_{23} \\ \bar{\gamma}^{cst}_{12} \\ \bar{\gamma}^{cst}_{13} \end{Bmatrix} \tag{22}$$

In this study, the boundary conditions of the finite element unit cell model are applied according to Sun and Vaidya (1995).

4.2.1. Calculation of $C^*_{11}(t)$ and $C^*_{12}(t)$

Since only normal loadings are needed and there are two axes of symmetry, only a quadrant of the original unit cell model as shown in Fig. 2 was used to calculate $C^*_{11}(t)$ and $C^*_{12}(t)$. The displacement constraints applied to the finite element models for calculating $C^*_{11}(t)$ and $C^*_{12}(t)$ are as follows:

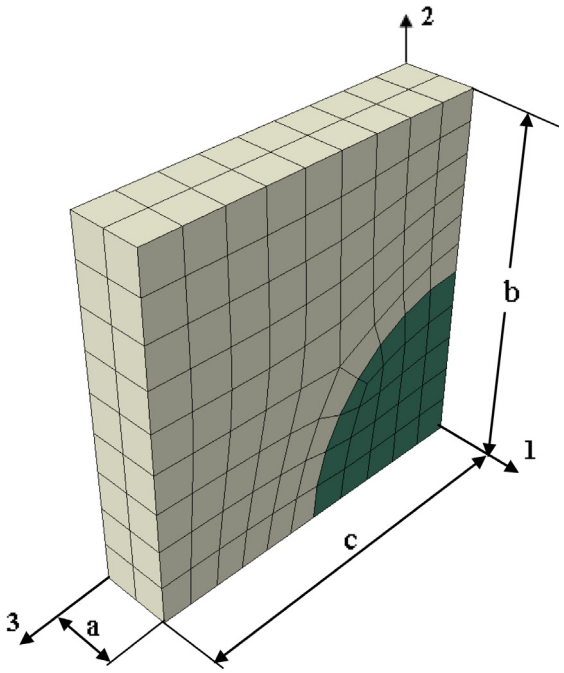

Fig. 2. Quadrant unit cell model used for the calculations of $C^*_{11}(t),\ C^*_{12}(t),\ C^*_{22}(t)$ and $C^*_{23}(t)$.

$$\begin{aligned}
&\boldsymbol{u_1}(0,2,3)=0\\
&\boldsymbol{u}_1(a,2,3)=\text{constant}=\delta\\
&\boldsymbol{u}_2(1,0,3)=0\\
&\boldsymbol{u}_2(1,b,3)=0\\
&\boldsymbol{u}_3(1,2,0)=0\\
&\boldsymbol{u}_3(1,2,c)=0
\end{aligned} \tag{23}$$

where $\boldsymbol{u}_1$, $\boldsymbol{u}_2$, and $\boldsymbol{u}_3$ represent the displacements in the 1-, 2- and 3-directions, respectively. The $C^*_{11}(t)$ and $C^*_{12}(t)$ are computed as

$$C^*_{11}(t)=\frac{\bar{\sigma}_{11}(t)}{\bar{\varepsilon}^{\text{cst}}_{11}} \quad C^*_{12}(t)=\frac{\bar{\sigma}_{22}(t)}{\bar{\varepsilon}^{\text{cst}}_{11}} \tag{24}$$

where $\bar{\varepsilon}^{\text{cst}}_{11}=\delta/a$; $\bar{\sigma}_{11}(t)$ and $\bar{\sigma}_{22}(t)$ are generated due to the boundary conditions in Eq. (23).

4.2.2. Calculation of $C^*_{22}(t)$ and $C^*_{23}(t)$

The quadrant unit cell model shown in Fig. 2 was also used for the calculations of $C^*_{22}(t)$ and $C^*_{23}(t)$. The displacement constraints applied to the finite element models for calculating $C^*_{22}(t)$ and $C^*_{23}(t)$ are as follows:

$$\begin{aligned}
&\boldsymbol{u}_1(0,2,3)=0\\
&\boldsymbol{u}_1(a,2,3)=0\\
&\boldsymbol{u}_2(1,0,3)=0\\
&\boldsymbol{u}_2(1,b,3)=\text{constant}=\delta\\
&\boldsymbol{u}_3(1,2,0)=0\\
&\boldsymbol{u}_3(1,2,c)=0
\end{aligned} \tag{25}$$

The $C^*_{22}(t)$ and $C^*_{23}(t)$ are computed as

$$C^*_{22}(t)=\frac{\bar{\sigma}_{22}(t)}{\bar{\varepsilon}^{\text{cst}}_{22}} \quad C^*_{23}(t)=\frac{\bar{\sigma}_{33}(t)}{\bar{\varepsilon}^{\text{cst}}_{22}} \tag{26}$$

where $\bar{\varepsilon}^{\text{cst}}_{22}=\delta/b$; $\bar{\sigma}_{22}(t)$ and $\bar{\sigma}_{33}(t)$ are generated due to the boundary conditions in Eq. (25).

4.2.3. Calculation of $C^*_{44}(t)$

A two dimensional plane strain model as shown in Fig. 3 was employed to compute the transverse stress relaxation modulus $C^*_{44}(t)$. The required displacement constraints are as follows

$$\begin{aligned}
&\boldsymbol{u}_2(-b,3)=\boldsymbol{u}_2(b,3)\\
&\boldsymbol{u}_3(-b,3)=\boldsymbol{u}_3(b,3)\\
&\boldsymbol{u}_2(2,-c)=\boldsymbol{u}_2(2,c)\\
&\boldsymbol{u}_3(2,-c)=\boldsymbol{u}_3(2,c)
\end{aligned} \tag{27}$$

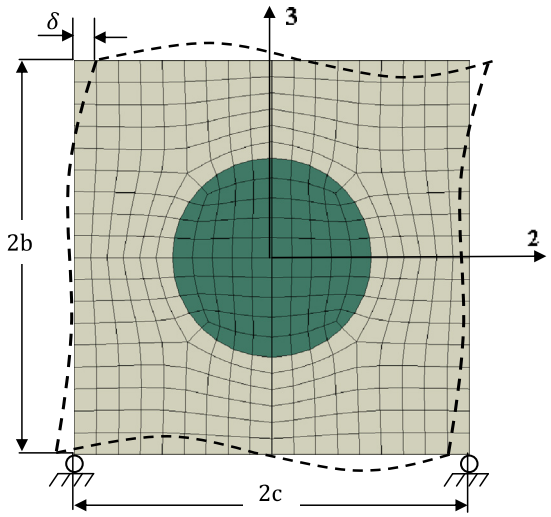

Fig. 3. Two dimensional model used to calculate the transverse stress relaxation modulus $C^*_{44}(t)$.

The further constraints are

$$\varepsilon_{33}(\pm b, 3) = 0 \quad \varepsilon_{22}(2, \pm c) = 0 \tag{28}$$

The bottom corners are placed on rollers to eliminate rigid body displacement. A constant horizontal displacement δ is applied to each corner of the unit cell. The $C^*_{44}(t)$ is obtained as

$$C^*_{44}(t) = \frac{\bar{\sigma}_{23}(t)}{\bar{\gamma}^{\text{cst}}_{23}} \tag{29}$$

where the constant global transverse shear strain $\bar{\gamma}^{\text{cst}}_{23} = \delta/c$.

4.2.4. Calculation of $C^*_{55}(t)$

The calculation of average longitudinal stress relaxation modulus $C^*_{55}(t)$ is performed on a 3D full unit cell model as shown in Fig. 4. The required displacement constraints are as follows

$$\begin{aligned}
&\boldsymbol{u}_1(0,2,3) = \boldsymbol{u}_1(a,2,3)\\
&\boldsymbol{u}_2(0,2,3) = \boldsymbol{u}_2(a,2,3)\\
&\boldsymbol{u}_3(0,2,3) = \boldsymbol{u}_3(a,2,3)\\
&\boldsymbol{u}_1(1,2,0) = \boldsymbol{u}_2(1,2,0) = \boldsymbol{u}_3(1,2,0) = 0\\
&\boldsymbol{u}_1(1,2,2c) = \text{constant} = \delta\\
&\boldsymbol{u}_3(1,2,2c) = 0
\end{aligned} \tag{30}$$

The $C^*_{55}(t)$ is calculated as

$$C^*_{55}(t) = \frac{\bar{\sigma}_{12}(t)}{\bar{\gamma}^{\text{cst}}_{12}} \tag{31}$$

where the constant global transverse shear strain $\bar{\gamma}^{\text{cst}}_{12} = \delta/2c$.

In all finite element simulations, the constant strains were instantaneously applied at $t = 0$ and then kept constant until the end of simulations as described by Eq. (2).

4.3. Predictions of effective stress relaxation stiffness

The effective stress relaxation coefficients predicted by the VAMUCH model and ABAQUS finite element models are plotted in Figs. 5–10. It is obviously observed that the VAMUCH predictions are almost identical to ABAQUS results. The accuracy

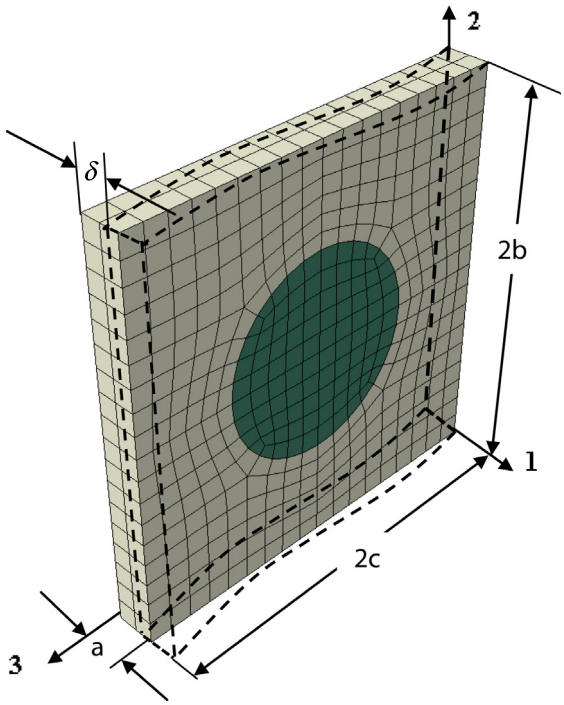

Fig. 4. Full finite element unit cell model used for the calculation of effective longitudinal stress relaxation modulus $C^*_{55}(t)$.

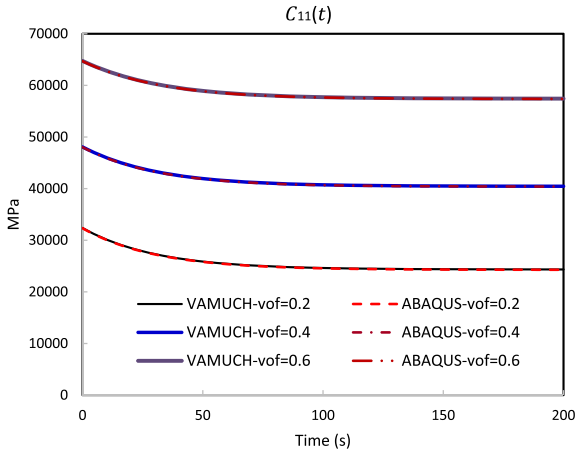

Fig. 5. Variation of effective stress relaxation coefficient $C^*_{11}(t)$ with respect to time for different volume fraction of the fibers.

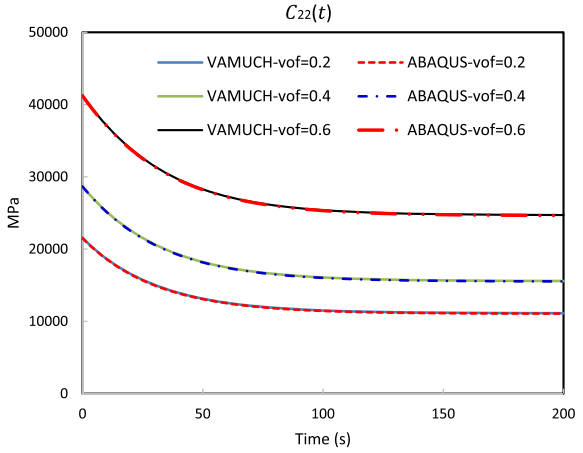

Fig. 6. Variation of effective stress relaxation coefficient $C^*_{22}(t)$ with respect to time for different volume fraction of the fibers.

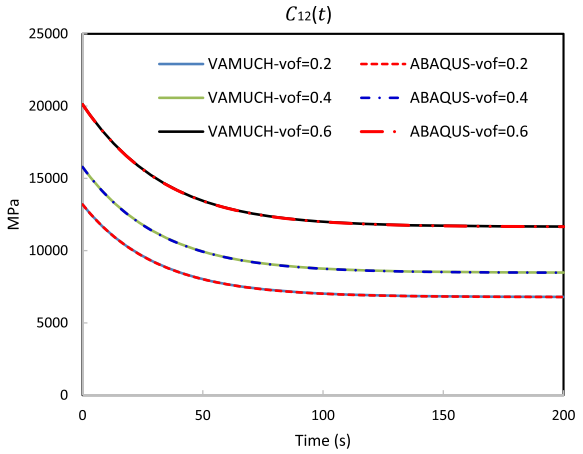

Fig. 7. Variation of effective stress relaxation coefficient $C^*_{12}(t)$ with respect to time for different volume fraction of the fibers.

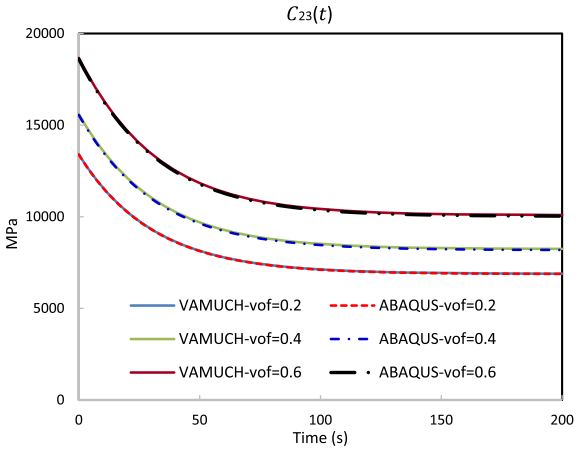

Fig. 8. Variation of effective stress relaxation coefficient $C^*_{23}(t)$ with respect to time for different volume fraction of the fibers.

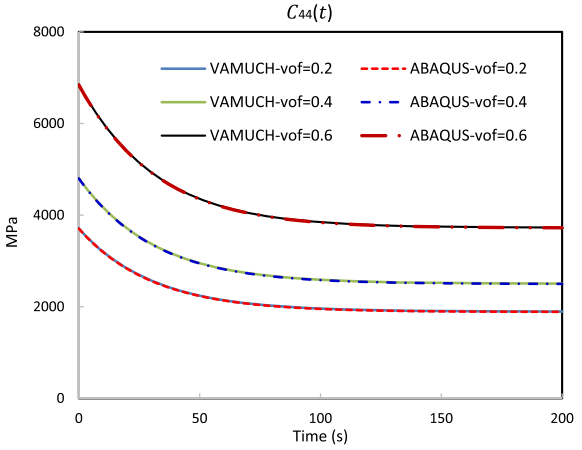

Fig. 9. Variation of effective stress relaxation coefficient $C^*_{44}(t)$ with respect to time for different volume fraction of the fibers.

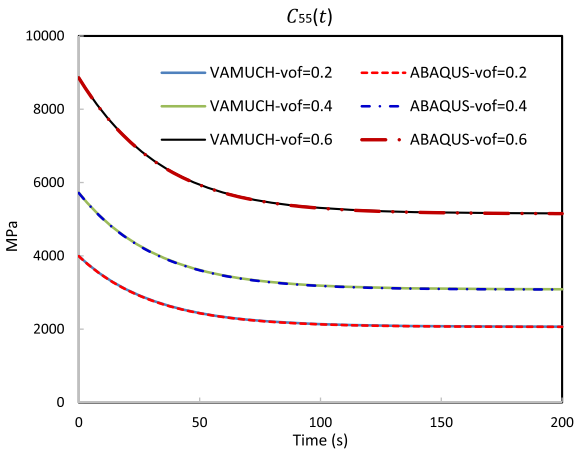

Fig. 10. Variation of effective stress relaxation coefficient $C^*_{55}(t)$ with respect to time for different volume fraction of the fibers.

of the VAMUCH model has been validated by ABAQUS finite element models. VAMUCH can obtain the complete set of effective instantaneous coefficients within one step of analysis while the predictions obtained by ABAQUS require multiple running on multiple loading and boundary conditions. When calculating the effective properties of fiber reinforced composites,

VAMUCH only need the mesh information (such as the number of nodes and elements, and the coordinate of nodes) of a 2D model as shown in Fig. 3 but different model geometries as shown in Figs. 2–4 are needed when using ABAQUS finite element modeling technique. Hence, VAMUCH is more efficient than ABAQUS finite element models.

5. Conclusions

A micromechanics model has been developed to calculate the effective stress relaxation stiffness of linear viscoelastic composites. This model possesses the advantages of geometrical flexibility and can obtain the complete of effective coefficients within one step of analysis. Hence, it can be applied to polymer composites having any shapes of reinforcements although a fiber reinforced composites was used as a numerical example in this work. The predictions of effective stress relaxation stiffness are obtained in the time domain without applying the traditionally used Laplace transform and inversion and correspondence principle.

References

Abadi, M. T. (2009). Micromechanical analysis of stress relaxation response of fiber-reinforced polymers. *Composites Science and Technology, 69*, 1286–1292.

Aboudi, J. (2000). Micromechanical modeling of finite viscoelastic multiphase composites. *Mathematical Physics, 54*, 114–134.

Barbero, E. J., & Luciano, R. (1995). Micromechanical formulas for the relaxation tensor of linear viscoelastic composites with transversely isotropic fibers. *International Journal of Solids and Structures, 32*(13), 1859–1872.

Barbero, E.J. (1994). Construction: Applications and design, Lubin's handbook of composites (2nd ed.).

Benveniste, Y. (1987). A new approach to the application of Mori–Tanka's theory in composite materials. *Mechanics of Materials, 6*, 147–157.

Brinson, L. C., & Lin, W. S. (2003). Comparison of micromechanics methods for effective properties of multiphase viscoelastic composites. *Composite Structures, 41*, 353–367.

Christensen, R. M. (1979). *Mechanics of composite materials*. Mineola, New York: Dover Publications, Inc.

Fisher, F. T., & Brinson, L. C. (2003). Viscoelastic interphase in polymer-matrix composites: Theoretical models and finite element analysis. *Composites Science and Technology, 61*, 731–748.

Haasemann, G., & Ulbricht, V. (2009). Numerical evaluation of the viscoelastic and viscoplastic behavior of composites. *Tchnishe Mechanik, 30*(1-3), 122–135.

Hashin, Z. (1965). Viscoelastic behavior of heterogeneous media. *Journal of Applied Mechanics, Transactions ASME, 32*(3), 630–636.

Hashin, Z. (1970). Complex moduli of viscoelastic composites-I. General theory and application to particulate composites. *International Journal of Solids and Structures, 6*, 539–552.

Hashin, Z. (1970). Complex moduli of viscoelastic composites-I. General theory and application to particulate composites. *International Journal of Solids and Structures, 6*, 797–807.

Hashin, Z. (1983). Analysis of composite materials-a survey. *Journal of Applied Mechanics, 105*, 481–504.

Levin, V., & Sevostianov, I. (2005). Micromechanical modeling of the effective viscoelastic properties of inhomogeneous materials using fraction-exponential operators. *International Journal of Fracture, 134*, L37–L44.

Li, K., Gao, X. L., & Roy, A. K. (2006). Micromechanical modeling of viscoelastic properties of carbon nanotube-reinforced polymer composites. *Mechanics of Advanced Materials and Structures, 13*, 317–328.

Megnis, M., Varna, J., Allen, D. H., & Holmberg, A. (2001). Micromechanical modeling of viscoelastic response of GMT composites. *Journal of Composite Materials, 35*, 849–882.

Mori, T., & Tanaka, K. (1973). Average stress in matrix and average elastic energy of materials with misfitting inclusions. *Acta Metallurgica, 21*, 571–574.

Naik, A., Abolfathi, N., Karami, G., & Ziejewski, M. (2008). Micromechanical viscoelastic characterization of fibrous composites. *Journal of Composite Materials, 42*, 1179–1204.

Nemat-Nasser, S., & Hori, M. (1993). *Micromechanics: Overall properties of heterogeneous materials*. Amsterdam: Elsevier Science.

Park, S. W., & Schapery, R. A. (1999). Method of interconversion between linear viscoelastic material functions. Part I – A numerical method based on Prony series. *International Journal of Solids and Structures, 36*, 1653–1675.

Schapery, R. A. (1967). Stress analysis of viscoelastic composite materials. *Journal of Composite Materials, 1*, 228–267.

Sun, C. T., & Vaidya, R. S. (1995). Prediction of composite properties from a representative volume element. *Composites Science and Technology, 56*, 171–179.

Wang, Y. M., & Weng, G. J. (1992). The influence of inclusion shape on the overall viscoelastic behavior of composites. *Journal of Applied Mechanics, Transactions ASME, 112*, 157–163.

Yancey, R. N., & Pindera, M.-J. (1990). Micromechanical analysis of the creep response of unidirectional composites. *Journal of Engineering Materials and Technology, 112*, 157–163.

Yu, W., & Tang, T. (2007). Variational asymptotic method for unit cell homogenization of periodically heterogeneous materials. *International Journal of Solids and Structures, 44*, 3738–3755.